Analysis of a Fiber Bragg Grating Writing Process using Low-Coherence Interferometry and Layer-Peeling

R.J. Espejo, M. Svalgaard, and S.D. Dyer
National Institute of Standards and Technology
Optoelectronics Division
325 Broadway, Boulder, CO 80305 USA
email: espejo@boulder.nist.gov

Abstract: *We demonstrate accurate measurements of the longitudinal refractive index profile of a fiber Bragg grating (FBG). We measure the impulse response of a FBG with a low-coherence interferometer, calculate the complex spectrum from a Fourier transform of the interferogram, and then apply a layer-peeling algorithm to find the index profile of the measured FBG. We use our results to calibrate and identify systematic errors in a scanning beam/dithered phase mask FBG writing system.*

1. Introduction

A written fiber Bragg grating (FBG) is often analyzed by the examination of the reflected power spectrum. This does little to indicate the origins of errors that can degrade the spectral quality. Systematic problems with the writing system such as phase-mask imperfections are difficult to diagnose in this manner. Thus writing often involves a process of trial and error, ending when the correct spectrum is achieved.

Better quality control of the writing process can be accomplished by measuring the FBG's index profile. The exact index profile is particularly important in cases of complicated index profiles, where small deviations from design can greatly affect the resulting spectra. Knowledge of the actual longitudinal index profile that was written into the FBG can be used to identify problems that can then be corrected or compensated for in subsequent writings [1]. This has the potential to greatly improve the quality of the FBGs produced.

We use low-coherence interferometry (LCI) to measure the impulse response of the grating. A layer-peeling algorithm is then used to calculate the complex spatial coupling coefficient of the FBG. We show that our measurements can be used to calibrate a scanning beam/dithered phase mask writing system, and that we can identify systematic errors in written FBGs.

2. Measurement System

The impulse response of the FBG is measured using the fiber-optic Michelson LCI, shown in Fig. 1. We have previously shown that accurate, high-resolution measurements of the dispersive and spectral properties of optical components can be achieved using this measurement system [2].

The FBG to be measured (DUT) is placed in one arm of the Michelson LCI along with a 1319 nm reference grating. The other arm has a variable air path that is capable of scanning a total distance of 1.4 m. The low-coherence signal is provided by a commercial C+L band superfluorescent source. A 1319 nm reference laser tracks the interferometer's total optical path difference as the reference arm mirror is translated. The reference grating

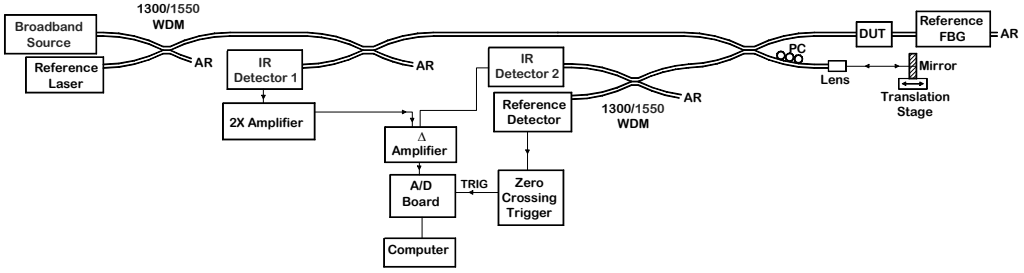

Figure 1. *Low-coherence measurement system. DUT: device under test. AR: anti-reflection. PC: polarization control. WDM: wavelength division multiplexer.*

provides a narrowband reflection of just the reference laser signal. The low-coherence signal is differentially detected and then digitized with a 16-bit A/D card. Triggering occurs at every zero crossing of the interference signal created by the reference laser, which sets the sample spacing to 659.5 nm. The signal-to-noise ratio (SNR) is greater than 70 dB.

The complex reflection spectrum is found by calculating the fast Fourier transform (FFT) of the interferogram. A layer-peeling algorithm is then applied to the calculated complex spectrum to determine the complex coupling coefficient of the FBG, *q(z)* [3]. The index modulation amplitude, Δn_{ac}, is calculated from *q(z)* as follows:

$$\Delta n_{ac}(z) = \frac{|q(z)|\lambda_B}{\pi\eta}, \tag{1}$$

where λ_B is the Bragg wavelength and η is the fraction of power in the fiber core. Assuming that the spatial grating phase is constant, as is ideally the case for a phase mask, the average index change, Δn_{dc}, can be found by

$$\Delta n_{dc}(z) = \frac{\lambda_B}{2\eta}\left(\frac{1}{\Lambda_B} - \frac{1}{\Lambda_{eff}(z)}\right), \tag{2}$$

where Λ_B is the Bragg period, and the effective grating period Λ_{eff} is determined from

$$\Lambda_{eff}(z) = \Lambda_B\left(1 + \frac{\Lambda_B}{2\pi}\frac{d}{dz}\arg(q(z))\right)^{-1}. \tag{3}$$

The physical interpretation of these grating parameters is shown in Fig. 2.

The spatial resolution of the calculated FBG index profile is limited by the bandwidth of the low-coherence source [3]. A spectral width of 1525 nm-1610 nm gives a maximum resolution of 15 μm.

3. Calibration of Δn_{ac} as a Function of Phase Mask Dither Voltage

It has been shown that an effective method for controlling the FBG profile during writing is by scanning a narrow ultraviolet (UV) beam across a phase-mask (PM) while the position of the PM is dithered by a piezoelectric transducer (PZT) [4]. Dithering of the PM with an amplitude of one-half the mask period has the effect of completely washing out the fringe visibility; therefore we can control the index modulation written into the fiber by changing the PM dither voltage as the writing beam is scanned across the fiber.

The dither voltage applied to the PZT affects the Δn_{ac} in a cosinusoidal manner, with the period of the cosine determined by the PM period and the PZT's response [4]. These variables necessitate a calibration of the dither voltage applied to the PZT in order to have accurate control over Δn_{ac} for a particular writing system.

To obtain this calibration we wrote a series of gratings with equal exposure times but different dither voltages along a single fiber. The measured Δn_{ac} for each grating is shown in Fig. 3a. In Fig. 3b we show the peak Δn_{ac} of each grating as a function of the dither voltage that was applied when that grating was written. The peak Δn_{ac} of each grating is normalized to the maximum possible index modulation amplitude, which occurs when no dither is applied. We calculated a least-squares cosinusoidal curve fit to the measured data using the cosine period as the free parameter in the fit. Figure 3b allows us to predict the dither voltage needed to achieve a desired Δn_{ac}. By varying the dither voltage as the UV writing beam is scanned along the fiber, gratings with a wide variety of index modulation profiles can be written.

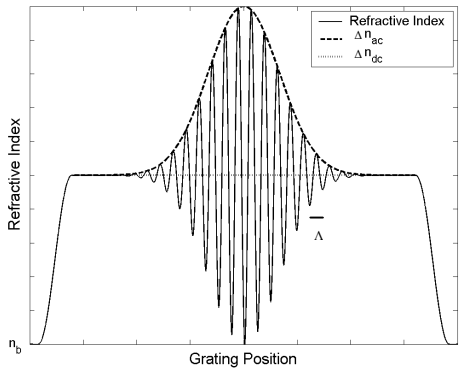

Figure 2. *Physical interpretation of Δn_{ac}, Δn_{dc}, and Λ of a FBG. An un-chirped Gaussian apodized FBG shown. The modulation frequency is not shown to scale. n_b: fiber bulk index.*

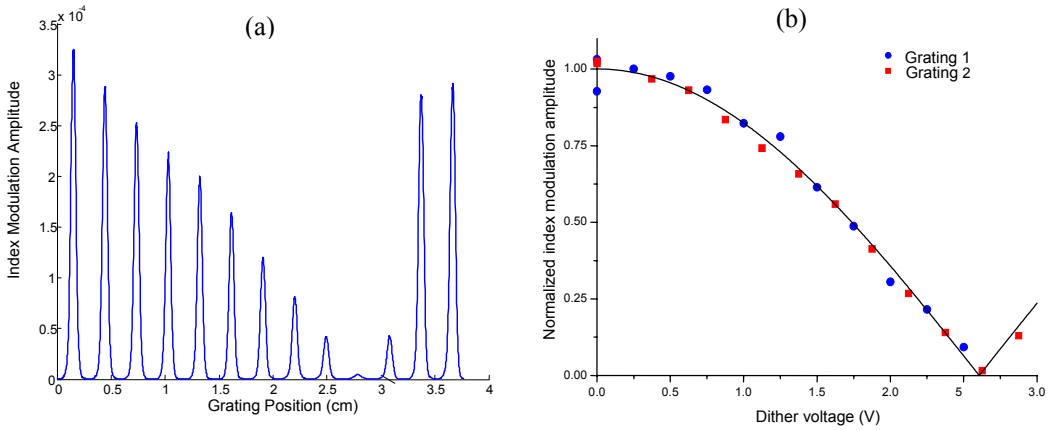

Figure 3. *(a): Measured Δn_{ac} of the grating series. Each grating has the same exposure; only the PZT dither amplitude is changed, and each is the width of the writing beam (~0.5 mm). Shown is the average of 10 measurements. (b) Index modulation (Δn_{ac}) vs. PM PZT dither voltage. Calibration curve fit is used for determining the appropriate dither voltage needed in order to achieve a desired index modulation when writing a FBG. Two separate grating sets fabricated several weeks apart were used.*

4. Troubleshooting Errors in the Grating Writing Process

Our measurements can be used to identify problems in the grating fabrication process, which can lead to unexpected errors in the reflection spectrum of a written FBG. Once these problems are identified and characterized they can then be compensated and the desired spectrum achieved.

4.a. Phase Mask Uniformity

To check the PM for non-uniformities 18 gratings were written under identical conditions across the full width of the mask. Sampling of the PM in this manner was chosen rather than writing a single uniform grating, due to the difficulties in measuring long, strong gratings [5].

The measured Δn_{ac} is shown in Fig. 4. The slight non-uniformity shows a similar trend as seen in direct measurements of the diffraction efficiencies for this mask. Our results show that the achieved index modulation amplitude decreases in a slow manner across the phase mask, with a total variation of ~8 %. After mapping the PM non-uniformity, we can adjust the PM dither voltage or the UV exposure time when writing subsequent gratings with the same PM to compensate for its non-uniformity.

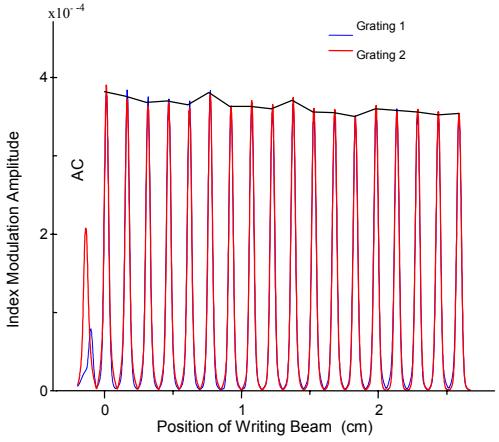

Figure 4. *Grating series for mapping phase-mask non-uniformity. For the peak labeled AC (alignment check) the beam was walked on to the edge of the mask to ensure that the writing began in the same place each time. Two different grating sets were used and the results for each are shown. The two curves are practically indistinguishable.*

4. b. Writing Errors

Cosine-apodized FBGs are desirable since their reflection spectra have suppressed side-lobes. We produced a cosine-apodized grating using our scanning beam/dithered PM writing system. The measured spectrum and index profile for this grating are shown in Figs. 5a and b. Although the measured Δn_{ac} fits the intended cosine curve reasonably well, several obvious imperfections can be seen. The one that is labeled "mask defect" appears to be a defect on the PM since it appears in the same location on several other gratings written with this mask. The second, narrow grating seen to the right of the main grating labeled "writing error" is the result of an error that occurred when the writing beam was not shuttered at the appropriate

time. Figure 5b shows the Δn_{dc} of the FBG. An ideal apodized FBG should have a constant dc component to its index profile. The linear increase of approximately 7.8×10^{-5} /cm in Δn_{dc} detected in the measured FBG will cause a chirped broadening of the reflection spectrum

We simulated the combined effect of these writing errors on the FBG reflection spectrum using the well known matrix-transfer method [3]. The simulated spectrum is shown in Fig 5c along with the reflection spectrum of an ideal cosine-apodized grating and the reflection spectrum measured by LCI. The measured index profile of the FBG provides valuable information as to why the reflection spectrum does not match the ideal case. It is unlikely that these errors could have been identified by spectral analysis alone.

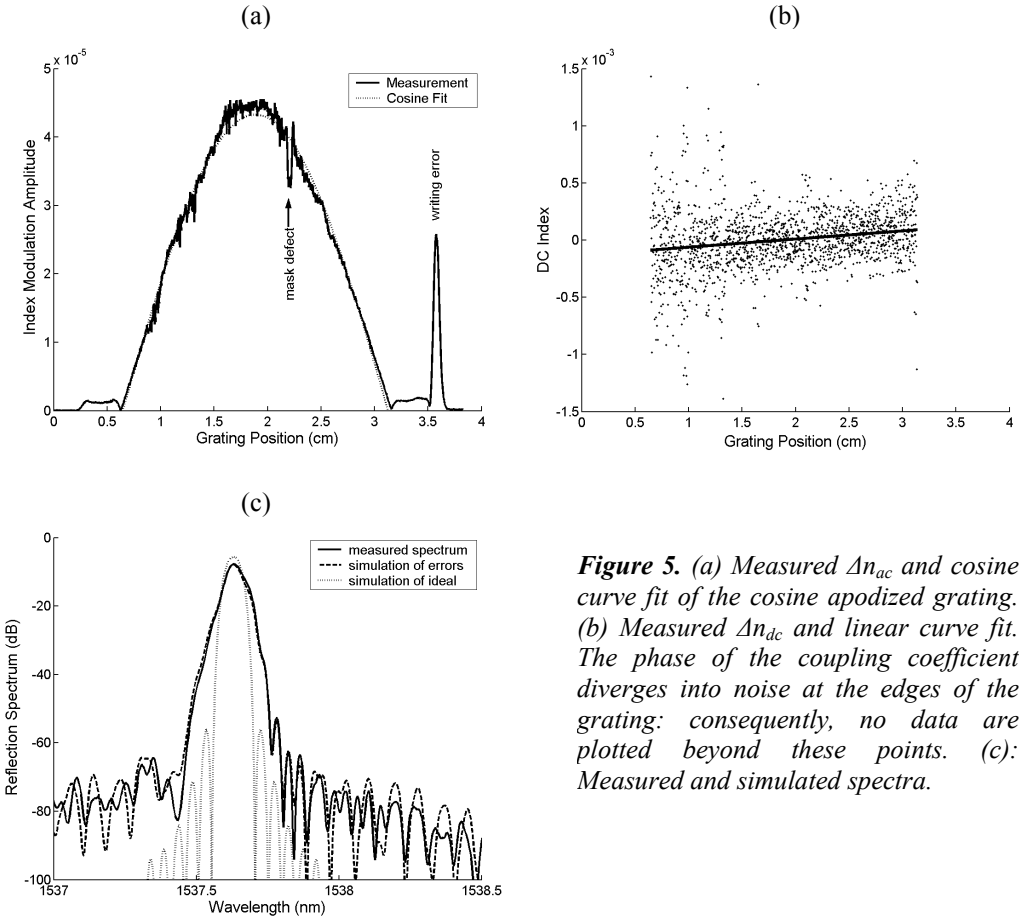

Figure 5. *(a) Measured Δn_{ac} and cosine curve fit of the cosine apodized grating. (b) Measured Δn_{dc} and linear curve fit. The phase of the coupling coefficient diverges into noise at the edges of the grating: consequently, no data are plotted beyond these points. (c): Measured and simulated spectra.*

5. Conclusion

We have demonstrated a fast and accurate method for the calibration and analysis of a FBG writing process. Our measurement gives high-resolution (15 μm) spatial characterization of the FBG. We have also shown the ability to identify imperfections in the written grating, and we have shown that these imperfections can have a significant impact on the FBG's reflection spectrum.

6. References.

1. A. V. Buryak and D.Y. Stepanov, "Correction of systematic errors in the fabrication of fiber Bragg gratings," *Opt. Lett*., vol. 27, no. 13, pp.1099-1101 (2002).
2. S.D. Dyer, R.J. Espejo, and P.A. Williams, "High-Resolution Group Delay Measurements of a Hydrogen Cyanide Gas Cell Using Low-Coherence Interferometry," SOFM 2002, Boulder, CO, NIST Spec. Publ. 988, pp. 45-48 (2002).
3. J. Skaar, L. Wang, and T. Erdogan, "On the Synthesis of Fiber Bragg Gratings by Layer Peeling," *IEEE J. Quan. Elect.*, vol. 37, no. 2, pp. 165-173 (2001).
4. M. J. Cole, W. H. Loh, R. I. Laming, M. Zervas and S. Barcelos, "Moving fibre/phase mask-scanning beam technique for enhanced flexibility in producing fibre gratings with a uniform phase mask," *Elect. Lett.*, vol. 31, pp. 1488-1490 (1995).
5. J. Skaar and R. Feced, "Reconstruction of gratings from noisy reflection data," *J. Opt. Soc. Am. A*, vol. 19, no. 11, pp. 2229-2237 (2002).